The Astrophysical Journal, 638:391–396, 2006 February 10

DIAGNOSING THE OUTFLOW FROM THE SGR 1806−20 GIANT FLARE WITH RADIO OBSERVATIONS

J. Granot,[1] E. Ramirez-Ruiz,[2] G. B. Taylor,[1,3] D. Eichler,[4] Y. E. Lyubarsky,[4] R. A. M. J. Wijers,[5]
B. M. Gaensler,[6] J. D. Gelfand,[6] and C. Kouveliotou[7]
Received 2005 March 15; accepted 2005 August 29

ABSTRACT

On 2004 December 27, the soft gamma repeater (SGR) 1806−20 emitted the brightest giant flare (GF) ever detected from an SGR. This burst of energy, which resulted in an (isotropic) energy release ∼100 times greater than the only two other known SGR GFs, was followed by a very bright, fading radio afterglow. Extensive follow-up radio observations provided a wealth of information with unprecedented astrometric precision, revealing the temporal evolution of the source size, along with densely sampled light curves and spectra. Here we expand on our previous work on this source, by explaining these observations within one self-consistent dynamical model. In this scenario, the early radio emission is due to the outflow ejected during the GF energizing a thin shell surrounding a preexisting cavity, where the observed steep temporal decay of the radio emission seen beginning on day 9 is attributed to the adiabatic cooling of the shocked shell. The shocked ejecta and external shell move outward together, driving a forward shock into the ambient medium, and are eventually decelerated by a reverse shock. As we show in a separate work by Gelfand and coworkers, the radio emission from the shocked external medium naturally peaks when significant deceleration occurs and then decays relatively slowly. The dynamical modeling of the collision between the ejecta and the external shell, together with the observed evolution of the source size (which is nicely reproduced in our model), suggests that most of the energy in the outflow was in mildly relativistic material, with an initial expansion velocity $v/c \lesssim d_{15}(1+d_{15}^2)^{-1/2} \sim 0.7$, for a distance of $15d_{15}$ kpc to SGR 1806−20. An initially highly relativistic outflow would not have produced a long coasting phase at a mildly relativistic expansion velocity, as was observed.

Subject headings: hydrodynamics — ISM: bubbles — pulsars: individual (SGR 1806−20) — stars: flare — stars: neutron — stars: winds, outflows

1. INTRODUCTION

Soft gamma repeaters (SGRs) are believed to be magnetars—a small class of slowly spinning neutron stars with extremely high surface magnetic fields, $B \gtrsim 10^{15}$ G (Duncan & Thompson 1992; Kouveliotou et al. 1998). They were discovered through their transient X-ray outbursts, during which they emit hundreds of short (∼0.2 s), soft ($kT \sim 25$ keV) bursts; very rarely (only twice so far), SGRs emit giant flares (GFs), extreme events with luminosities upwards of 10^{44} ergs s^{-1}. SGR 1806−20 lies in the Galactic plane, at a distance of about $d = 15d_{15}$ kpc (Corbel & Eikenberry 2004; Cameron et al. 2005; McClure-Griffiths & Gaensler 2005). The third GF yet recorded occurred on 2004 December 27, when SGR 1806−20 emitted a burst so extreme that it was the brightest extrasolar transient event ever recorded (Palmer et al. 2005; Hurley et al. 2005). The flare was also unique in creating a very bright radio afterglow (Gaensler et al. 2005; Cameron & Kulkarni 2005), which was monitored for months, providing an amazing wealth of data at several radio frequencies, including the temporal evolution of the source size and shape, polarization, and flux.

The data from the radio source that appeared in the aftermath of the GF provide a rare opportunity for a detailed study of a mildly relativistic blast wave, which might help bridge the gap between the relativistic outflows in cosmological gamma-ray bursts and supernova remnants. Gelfand et al. (2005) present a rebrightening episode in the radio light curve, which is well fit by a semianalytic spherical model in which the radio emission resulted from a blast wave driven by $\gtrsim 10^{24.5}$ g of baryonic material driven off the neutron star, and the expanding radio nebula has now entered its Sedov-Taylor phase of evolution. An accompanying study of the evolution of the size of the nebula confirms that it is indeed decelerating (Taylor et al. 2005). Furthermore, the motion of the flux centroid implies a predominantly one-sided mildly collimated outflow, i.e., a wide one-sided jet (Taylor et al. 2005).

In this paper, we expand on the framework laid out by Gaensler et al. (2005), Gelfand et al. (2005), and Taylor et al. (2005) and present a full dynamical model for the interaction of the outflow that was ejected during the 2004 December 27 GF with its surroundings, and in particular with an external shell. Our model, which is described in § 2, explains the large and diverse data sets for this event and constrains the initial velocity of the ejecta from the flare. Both a relativistic (§ 2.1) and a Newtonian (§ 2.2) outflow are considered. We find that only a Newtonian outflow with an initial expansion velocity $v \approx 0.7d_{15}c$ fits the observations well. In § 3 we derive the synchrotron emission implied by our dynamical model and show that it also agrees nicely with the radio observations. Our conclusions are discussed in § 4.

2. THE UNDERLYING DYNAMICS

The radio light curve initially exhibited a relatively moderate decay, $\sim t^{-1.5}$, followed by an achromatic steepening at $t_b \approx 9$ days after the GF, to $\sim t^{-2.7}$ (Gaensler et al. 2005). This was followed

[1] KIPAC, Stanford University, P.O. Box 20450, MS 29, Stanford, CA 94309; granot@slac.stanford.edu.
[2] Institute for Advanced Study, Einstein Drive, Princeton, NJ 08540; Chandra Fellow.
[3] National Radio Astronomy Observatory, P.O. Box O, Socorro, NM 87801.
[4] Department of Physics, Ben Gurion University, P.O. Box 653, Be'er Sheva 84105, Israel.
[5] Astronomical Institute "Anton Pannekoek," University of Amsterdam, Kruislaan 403, 1098 SJ, Amsterdam, Netherlands.
[6] Harvard-Smithsonian Center for Astrophysics, 60 Garden Street, Cambridge, MA 02138.
[7] NASA Marshall Space Flight Center, XD-12, NSSTC, 320 Sparkman Drive, Huntsville, AL 35805.

by a rebrightening starting at ∼25 days and peaking at $t_p \approx$ 33 days (Gelfand et al. 2005); the decay rate slowed significantly thereafter ($\sim t^{-1.1}$; J. D. Gelfand et al. 2005, in preparation).

The apparent expansion velocity, $v_{\rm ap} = \beta_{\rm ap} c$, of the nebula was initially fairly constant,[8] $\sim 0.4\ d_{15} c$, and decreased at $t_{\rm dec} \sim t_p$ (Taylor et al. 2005). This value of $v_{\rm ap}$ is for the geometrical mean of the semimajor and semiminor axes and assumes a double sided outflow. Under the latter assumption, $v_{\rm ap}$ along the semimajor and semiminor axes is $\sim 0.5 d_{15} c$ and $\sim 0.25 d_{15} c$, respectively. However, as the motion of the flux centroid implies that the SGR is located close to the edge of the image along the semimajor axis (Taylor et al. 2005), this implies $v_{\rm ap} \sim 1.0 d_{15} c$ for the leading edge of the one-sided outflow.

The true velocity (in units of c) of the emitting material near the edge of the image is $\beta = (1 - \Gamma^{-2})^{1/2} = \beta_{\rm ap}/(\sin\theta + \beta_{\rm ap}\cos\theta)$, where θ is the angle between its direction of motion and the line of sight. The minimal true velocity corresponding to a given observed value of $\beta_{\rm ap}$ is $\beta_{\rm min} = \beta_{\rm ap}(1 + \beta_{\rm ap}^2)^{-1/2}$ or $\Gamma_{\rm min}\beta_{\rm min} = \beta_{\rm ap}$ and is obtained for an angle $\theta_{\rm min}$ that satisfies $\cos\theta_{\rm min} = \beta_{\rm min}$. The same angle, $\cos\theta = \beta$, is where $\beta_{\rm ap}$ is maximal for a fixed β (and therefore $\beta_{\rm ap} = \Gamma\beta$ at the outer edge of the image of a spherical source expanding at a velocity β). Therefore, we expect $\Gamma\beta \sim \beta_{\rm ap}$, and in our case $\Gamma\beta \sim 1.0\ d_{15}$, so that $\beta \sim d_{15}(1 + d_{15}^2)^{-1/2}$ or $\beta \sim 0.7$ for $d_{15} \approx 1$.

Since the axis ratio of the radio image at the times relevant for our modeling is at most ∼2:1, and for the sake of simplicity, we adopt a spherical model for most of our analysis and later introduce the corrections for a mildly collimated one-sided outflow, as is implied by the observations.

As the source was already fading by the time of the first observation ($t_{\rm I} \approx 7$ days), the radio emission must have turned on at an earlier time and at a smaller radius. The radio spectrum and linear polarization observations suggest that we are seeing synchrotron emission. If the relativistic electrons that are emitting this radiation were accelerated at a much smaller radius ($\ll 10^{16}$ cm), then most of their energy would have been lost via adiabatic cooling by $t_{\rm I}$, thus dramatically increasing the GF energy requirements. Moreover, the achromatic light curve steepening at t_b (Gaensler et al. 2005) strongly suggests a hydrodynamic transition at that time. A simple explanation for this overall behavior arises if the outflow from the GF initially coasted with negligible interaction with the ambient medium, until at $t_{\rm col} = 5 t_{\rm col,5}$ days it collided with a thin external shell, which caused it to decelerate by a reverse shock, while the external shell was accelerated by a forward shock.[9] After this collision the two shells move together at a somewhat reduced speed. Thus, the emission up to t_b is dominated by the *recently* shocked electrons in these two shells. The radiation then arrives at the observer at a time $t \lesssim 2 t_{\rm col}$ due to light travel effects and the finite time it takes for the shock to cross the shells. At $t > t_b$ the emission is dominated by the adiabatically cooling electrons in the two shells. As shown in § 3 (see also Gaensler et al. 2005), this naturally produces the unusually steep decay in the light curve.

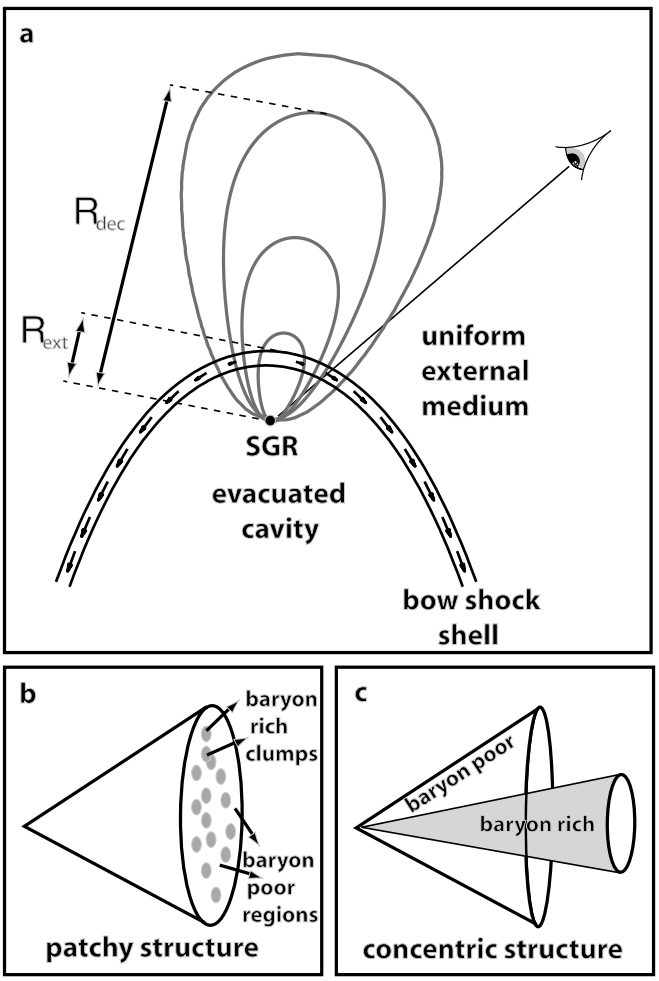

FIG. 1.—Illustration of the basic underlying geometry in our model. (*a*) A preexisting shell surrounding a cavity (i.e., an evacuated region) is possibly formed due to the interaction of the SGR quiescent wind with the external medium, and the SGR's supersonic motion relative to the external medium. The outflow from the SGR 1806−20 December 27 giant flare was ejected mainly in one preferred direction, probably not aligned with the head of the bow shock (which is in the direction of the SGR's systemic motion). The ejecta collide with the external shell at a radius $R_{\rm ext}$, and then the merged shell of shocked ejecta and shocked swept up external shell keeps moving outward at a constant (mildly relativistic) velocity. As it coasts outward, it gradually sweeps the external medium until at a radius $R_{\rm dec} \sim (4-5) R_{\rm ext}$ it sweeps up a sufficient mass of external medium in order to decelerate significantly. At $R > R_{\rm dec}$ the structure of the flow gradually approaches the spherical self-similar Sedov-Taylor solution. (*b*, *c*) Most of the mass in the outflow was in baryons that were decoupled from most of the radiation, and our line of sight was baryon-poor. This naturally occurs if there are separate baryon-rich (radiation-poor) and baryon-poor (radiation-rich) regions. Such regions might consist of small baryon-rich clumps surrounded by baryon-poor regions (*b*) or might alternatively be part of a global large-scale, possibly concentric configuration (*b*).

As the merged shell expands outward, it drives a shock into the ambient medium. An increasing amount of external mass is swept up, until the emission from this shocked fluid starts dominating the light curve at $t \gtrsim 25$ days. This naturally produces a rebrightening in the light curve that peaks at $t_p \approx 33$ days (Gelfand et al. 2005); as expected, a decrease in the expansion velocity was observed at about the same time, $t_{\rm dec} \sim t_p$ (Taylor et al. 2005). At $t > t_{\rm dec}$ the hydrodynamics gradually approach the self-similar Sedov-Taylor solution, which predicts a slower flux decay rate, in agreement with observations (Gelfand et al. 2005). An outline of our basic picture is shown in Figure 1*a*. Below we reproduce the main observed features using a simple

[8] We adopt the value that was derived by Taylor et al. (2005) for the average expansion velocity during the first 82 days, which is slightly higher than the value reported initially by Gaensler et al. (2005).

[9] Such a shell surrounding a preexisting cavity is thought to be formed behind the bow shock due to the supersonic motion of SGR 1806−20 through the ISM and its quiescent wind (Gaensler et al. 2005). Alternatively, it could also arise from an earlier and initially faster mass ejection from the SGR 1806−20 GF, which was decelerated by the external medium to a velocity slightly below that of the coasting second shell, thus causing the two shells to collide (the "refreshed shock" scenario; e.g., Granot et al. 2003).

analytic model for the interaction between the outflow and its surroundings, and we present a numerical simulation that broadly agrees with the analytic model and nicely reproduces the observed evolution of the source size.

2.1. *Relativistic Outflow*

A simple model for the collision between the cold ejecta shell of initial Lorentz factor $\Gamma_{\rm ej} = (1 - \beta_{\rm ej}^2)^{-1/2}$ and mass $M_{\rm ej}$, and an external thin shell of mass $M_{\rm ext}$ at rest at a radius $R_{\rm ext}$, is a plastic collision in which the two shells are shocked (the two shocked fluids separated by a contact discontinuity) and subsequently move together at $\Gamma_f = (1 - \beta_f^2)^{-1/2}$. Both $\Gamma_{\rm ej}$ and Γ_f are measured in the rest frame of the unperturbed external medium. Energy and momentum conservation in the rest frame of the merged shell require $E_f/c^2 = M_f = \Gamma_r M_{\rm ej} + \Gamma_f M_{\rm ext}$ and $\Gamma_r \beta_r M_{\rm ej} = \Gamma_f \beta_f M_{\rm ext}$, respectively, where $\Gamma_r = (1 - \beta_r^2)^{-1/2} = \Gamma_{\rm ej}\Gamma_f(1 - \beta_{\rm ej}\beta_f)$ is the initial Lorentz factor of the ejecta in the rest frame of the merged shell. The resulting internal energy is $E_{\rm int}/c^2 = (\Gamma_r - 1)M_{\rm ej} + (\Gamma_f - 1)M_{\rm ext}$, and the final velocity is

$$\frac{\beta_f}{\beta_{\rm ej}} = \left(1 + \frac{M_{\rm ext}}{\Gamma_{\rm ej} M_{\rm ej}}\right)^{-1}. \quad (1)$$

This shows that an external mass of $M_{\rm ext} \sim \Gamma_{\rm ej} M_{\rm ej}$ is required in order to significantly reduce the initial velocity.

For an *initially* relativistic outflow, $\Gamma_{\rm ej} \approx E/M_{\rm ej}c^2 \gg 1$ and $\beta_{\rm ej} \approx 1$, so that $\beta_f \approx (1 + M_{\rm ext}c^2/E)^{-1}$, which for $M_{\rm ext}c^2 \gg E$ (and correspondingly $\beta_f \ll 1$) gives $M_{\rm ext} v_f^2 \approx \beta_f E$. Therefore, in this limit, the kinetic energy of the merged shell carries only a small fraction ($\sim\beta_f$) of the total energy, while most of the energy is in the internal energy of the shocked ejecta ($E_{\rm int} \approx E \approx \Gamma_{\rm ej} M_{\rm ej} c^2$). The relativistically hot shocked ejecta can then convert most of its internal energy back into kinetic energy through $P\,dV$ work as the merged shell keeps expanding. This might initially (soon after the collision) accelerate the shell and later cause it to decelerate more slowly with time (and radius), thus increasing the radius at which it decelerates significantly, $R_{\rm dec}$, compared to its value for a cold shell with the same (post-collision) mass and velocity, $R_{\rm dec} \sim 2^{1/3} R_{\rm ext}$.

Nevertheless, even if all the original energy is back in the form of kinetic energy at $R_{\rm dec}$, then still $E/c^2 \approx M_{\rm dec}\beta_{\rm dec}^2 \approx \beta_f M_{\rm ext}$, where $M_{\rm dec} = M(R_{\rm dec}) \approx (4\pi/3)\rho_{\rm ext} R_{\rm dec}^3$ is the total mass (in the shells and swept-up external medium) at $R_{\rm dec}$, and $\beta_{\rm dec} = \beta(R_{\rm dec}) \approx 0.4\ d_{15} \gtrsim \beta_f$. Finally, $M_{\rm ext} \approx (4\pi/3)\rho_{\rm ext} R_{\rm ext}^3$ for most reasonable scenarios that produce an external shell, such as a bow shock (Wilkin 1996).[10] This gives

$$\left(\frac{R_{\rm dec}}{R_{\rm ext}}\right)^3 \approx \frac{M_{\rm dec}}{M_{\rm ext}} \approx \frac{\beta_f}{\beta_{\rm dec}^2} \lesssim \beta_{\rm dec}^{-1} \sim 2.5 d_{15}^{-1}. \quad (2)$$

We now proceed to compare the radio observations with the above calculations. The angular diameter of the source at the time of the first observation, $t_{\rm I} \approx 7$ days, and at the epoch of deceleration, $t_{\rm dec} \sim t_p \approx 33$ days, was about 80 and 300 mas, respectively.[11] The corresponding radii are $R_{\rm I} = 9.0 \times 10^{15} d_{15}$ cm and $R_{\rm dec} \approx 3.4 \times 10^{16} d_{15}$ cm. The requirement that $R_{\rm ext} < R_{\rm I}$ gives $R_{\rm dec}/R_{\rm ext} \gtrsim 3.75$ and therefore $(R_{\rm dec}/R_{\rm ext})^3 \approx 50(R_{\rm I}/R_{\rm ext})^3 \gtrsim 50$, which contradicts equation (2) for any reasonable value of d_{15}. Thus, an ultrarelativistic outflow ($\Gamma_{\rm ej} \gg 1$) fails to reproduce the observations, since $R_{\rm dec}$ would not be much larger than $R_{\rm ext}$; specifically, we expect $R_{\rm dec}/R_{\rm ext} \lesssim 1.4 d_{15}^{-1/3}$ (see eq. [2]).

2.2. *Newtonian Outflow*

For a Newtonian outflow ($\beta_{\rm ej} \ll 1$), equation (1) reduces to $\beta_f/\beta_{\rm ej} \approx M_{\rm ej}/M_f$, where $M_f \approx M_{\rm ej} + M_{\rm ext}$. Since $M(R_{\rm ext} < r < R_{\rm dec}) \sim M_f$ and $M_{\rm ext} \approx (4\pi/3)\rho_{\rm ext} R_{\rm ext}^3$, $M_{\rm ext} > M_{\rm ej}$ would imply $R_{\rm dec}/R_{\rm ext} \sim 2^{1/3} \approx 1.26$, in contrast with observations.

Therefore, we must have $M_{\rm ej} \gg M_{\rm ext}$, which results in $\beta_f \approx \beta_{\rm ej}$, $M_f \approx M_{\rm ej} \sim M_{\rm dec} \approx (4\pi/3)\rho_{\rm ext} R_{\rm dec}^3$, and $M_{\rm ej}/M_{\rm ext} \approx (R_{\rm dec}/R_{\rm ext})^3 \gtrsim 50$, or $R_{\rm ext} \approx (t_{\rm col}/t_{\rm I}) R_{\rm I} \approx 6.4 \times 10^{15} t_{\rm col,5} d_{15}$ cm and $M_{\rm ej}/M_{\rm ext} \approx (R_{\rm dec}/R_{\rm ext})^3 \approx 140 t_{\rm col,5}^{-3}$. At $t_{\rm dec}$ we directly measure the source size, $R_{\rm dec}$, and expansion velocity, $\beta_{\rm ej} \approx \beta_f \approx R_{\rm dec}/ct_{\rm dec} \approx 0.4 d_{15}$. Therefore, since the shocked external medium has comparable internal and kinetic energies, the energy in the outflow is given by $E \approx (4\pi/3)\rho_{\rm ext} R_{\rm dec}^3 v_{\rm ej}^2 \approx 3.8 \times 10^{46} n_0 d_{15}^5$ ergs and depends only on the unknown external density, $n_{\rm ext} = \rho_{\rm ext}/m_p = n_0$ cm^{-3}. Here $v_{\rm ej} = \beta_{\rm ej} c$ and $E_{46} = E/(10^{46}$ ergs). Thus, $n_0 \approx 0.26 d_{15}^{-5} E_{46}$ and $M_{\rm ej} \approx E/v_{\rm ej}^2 \approx 2.7 \times 10^{26} n_0 d_{15}^3$ g. These results for E and $M_{\rm ej}$ are similar to those derived by Gelfand et al. (2005).

A simple generalization for a wide one-sided jet is as follows. The volume of the shocked external fluid, and therefore its mass for a given external density, does not change. The kinetic energy per unit rest energy, $\Gamma - 1$, grows by a factor of $\sim$4–5 at the head of the jet (where $\Gamma\beta \approx 1$; see beginning of § 2) and decreases near the SGR. On average it increases by a factor of $\sim$2–3, and the estimate for $E/n_{\rm ext}$ increases by the same factor, while $M_{\rm ej}/n_{\rm ext}$ does not change.

Finally, it is important to keep in mind that the outflow might consist of more than one component. The simplest example is a relativistic shell (with $\Gamma \gg 1$) followed by a Newtonian shell (with $\Gamma\beta \lesssim 1$) that was ejected slightly later during the GF. The relativistic shell is shocked and decelerated to a Newtonian velocity as it collides with the external shell, at $t_{\rm col,1}$, while the Newtonian shell catches up and collides with the slower merged relativistic + external shell at $t_{\rm col,2} > t_{\rm col,1}$. As long as the velocity after the first collision is sufficiently smaller than that of the Newtonian shell, the subsequent dynamics would not be very different than for the Newtonian outflow case discussed above. An important difference, however, is that the emission would light up at $\sim t_{\rm col,1}/2\Gamma^2 \ll t_{\rm col,2}$, i.e., much earlier than without the relativistic component. (A similar result is also obtained if there is a continuous external medium instead of a shell surrounding a cavity.) Rapid follow-up observations of future GFs could test this hypothesis directly and teach us more about the properties of the outflow. In the present case, the later collision with the Newtonian shell might explain the change in the degree of linear polarization (from decreasing to increasing with time) and its position angle at $t \approx 10$ days (Gaensler et al. 2005).

We have tested the colliding shell scenario with the aid of numerical simulations, which model the dynamics much more accurately than the simple analytic model used above. Our basic

[10] This is an important assumption. If somehow the mass of the shell were larger by some factor $f = 3M_{\rm ext}/4\pi\rho_{\rm ext}R_{\rm ext}^3$, then $R_{\rm dec}/R_{\rm ext}$ would increase by a factor of $f^{1/3}$, so that $f \sim 10^2$ would be required in order to explain the observed evolution of the source size. Therefore, an external shell with $f \sim 10^2$, or alternatively a sharp density drop by a factor of $\sim 10^2$ around $R_{\rm ext}$ that lasts for at least an order of magnitude in radius, would in principle be consistent with the observations. In practice, however, such external density profiles seem highly contrived and therefore not very likely.

[11] At both epochs the image is somewhat elongated and the quoted value is along the semimajor axis (Gaensler et al. 2005; Taylor et al. 2005). The ratio of the angular size at these two epochs, however, is rather robust, and a comparable ratio is obtained along the semiminor axis. This ratio is also applicable for a one-sided outflow, as suggested in Taylor et al. (2005).

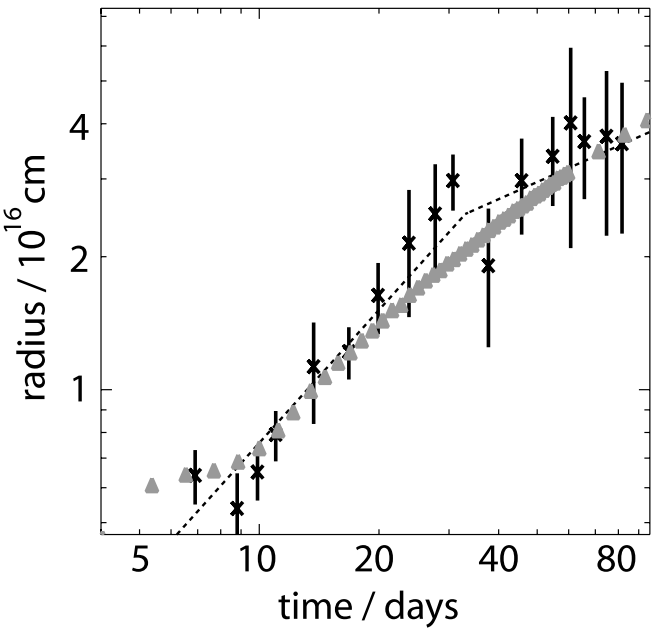

FIG. 2.—Temporal evolution of the observed size of the source from radio measurements (*asterisks*) of Taylor et al. (2005) assuming $d_{15} = 1$, together with the source size from our numerical simulation (*triangles*) and for our simple analytic model (*dotted line*). Our numerical simulation featured the collision between the outflow ejected during the SGR giant flare and a preexisting shell surrounding a cavity. The calculations were done in two-dimensional cylindrical coordinates for 10 levels of refinement using the piecewise parabolic method (PPM) adaptive mesh refinement code FLASH. The spherical initial configuration is as follows. In the inner region (outflow from the SGR, inner 5×10^{14} cm) both a thermal energy of $E = 10^{46}$ ergs and ejecta mass, $M_{\rm ej}$, are distributed uniformly; $M_{\rm ej}$ is selected so that $v = (2E/M_{\rm ej})^{1/2} \approx 0.4c$ (i.e., $M_{\rm ej} \approx 1.4 \times 10^{26}$ g). The injected gas and surrounding ISM (with $\rho_{\rm ext} = 2\times10^{-24}$ g cm^{-3}) are characterized by a 5/3 adiabatic index. More details will be presented in Ramirez-Ruiz et al. (2005, in preparation).

picture is confirmed by these calculations, and the observed evolution of the source size is nicely reproduced (see Fig. 2). The simple analytic expression for the source size is $R(t > t_{\rm col}) \approx R_{\rm dec}\min[(t/t_{\rm dec}),\ (t/t_{\rm dec})^{2/5}]$. The two asymptotic power laws correspond to the coasting phase and the Sedov-Taylor regime. A semianalytic model that gives a smooth transition between these two asymptotic power laws is presented in Figure 2 of Gelfand et al. (2005) and fitted to the source size as a function of time in Figure 2 of Taylor et al. (2005). Around the time of the collision, $t \sim t_{\rm col}$, there is a flat part in $R(t)$ due to the shocks that are crossing both shells. This flat part is nicely reproduced by the numerical simulation, and its exact shape depends on the details of the collision (and thus does not have a simple and robust analytic description). In a future work (E. Ramirez-Ruiz et al. 2005, in preparation) we investigate the dynamics in more detail, including the implications of aspherical outflows, which are relevant given the elongated nature of the radio image (Gaensler et al. 2005) and the motion of its flux centroid (Taylor et al. 2005).

3. EXPLAINING THE OBSERVED RADIO EMISSION

Once the reverse shock crosses the ejecta and the forward shock crosses the external shell, the supply of newly accelerated electrons will be exhausted. As the merged shells expand, the existing relativistic electrons cool adiabatically and the magnetic field decreases, thus nicely reproducing the sharp decay that was observed in the radio flux between 9 and ~25 days, $\sim t^{-2.7}$ Gaensler et al. (2005).

The emission from the forward shock is dominated by the newly shocked electrons, which are accelerated to relativistic energies with a power-law distribution, $dN/d\gamma_e \propto \gamma_e^{-p}$ for $\gamma_e > \gamma_m$. At $t < t_{\rm dec}$ the relative velocity of the shocked downstream fluid and the upstream fluid is roughly constant and equal to $v_{\rm rel} = \beta_{\rm rel}c \approx 0.3d_{15}c$ since $v_{\rm rel}/v_{\rm ej} \approx 3/4$. The average Lorentz factor of the relativistic electrons is given by $\langle\gamma_e\rangle = \epsilon_e e'/\xi_e n' m_e c^2$, where e' and n' are the proper internal energy density and number density of the shocked fluid, ϵ_e is the fraction of the postshock internal energy density in relativistic electrons, and ξ_e is the fraction of electrons that are accelerated to relativistic energies. The energy per proton is $e'/n' = (\Gamma_{\rm rel} - 1)m_p c^2 \approx (\beta_{\rm rel}^2/2)m_p c^2$, where the second expression is valid in the limit of a Newtonian blast wave. For $p > 2$ we have $\gamma_m = \langle\gamma_e\rangle(p-2)/(p-1)$ and therefore

$$\gamma_m = \frac{\epsilon_e}{\xi_e}\left(\frac{p-2}{p-1}\right)\frac{m_p}{m_e}\frac{\beta_{\rm rel}^2}{2} = 2g\xi_e^{-1}\epsilon_{e,-1}\left(\frac{\beta_{\rm rel}}{0.26}\right)^2, \quad (3)$$

where $g = 3(p-2)/(p-1)$ (=1 for $p = 2.5$), and $\epsilon_{e,-1} = \epsilon_e/0.1$. Since γ_m is the lowest Lorentz factor of the *relativistic* electrons, by definition $\gamma_m \gtrsim 2$. Gelfand et al. (2005) calculate the light curve under the assumption that $\epsilon_e/\xi_e =$ constant and $\gamma_m > 2$ (see also Frail et al. 2000), which is valid for $\epsilon_e > 0.1$ or $\xi_e \ll 1$ until there is significant deceleration. Once γ_m decreases to ~2, the subsequent behavior of ϵ_e and ξ_e depends on poorly understood shock acceleration of nonrelativistic electrons. Here it is assumed that $\epsilon_e =$ constant. Equation (3) shows that for $\epsilon_{e,-1} \lesssim 1$ (and it is difficult for ϵ_e to be much higher than 0.1) we have $\gamma_m \sim 2$, which is constant throughout, while $\xi_e \sim (v_{\rm rel}/v_{\rm ej})^2 \propto \beta_{\rm rel}^2$ decreases with time at $t \gtrsim t_{\rm dec}$. This results in a more moderate temporal decay of the flux at $t > t_{\rm dec}$ (see eq. [4]), in better agreement with observations.

At $t \gg t_{\rm dec}$ the shock dynamics approach the Sedov-Taylor self-similar solution, where $R \approx (Et^2/\rho_{\rm ext})^{1/5}$. Therefore, $v_{\rm rel}/v_{\rm ej} \approx (t_{\rm dec}/t)R/R_{\rm dec} \approx \min[1,\ (t/t_{\rm dec})^{-3/5}]$ and $v_{\rm sh,0}/v_{\rm ej} \approx v_{\rm sh,0}/v_f = 4/3$, where $t_{\rm dec} = R_{\rm dec}/v_{\rm sh,0} = (3E/2\pi\rho_{\rm ext}v_{\rm sh,0}^5)^{1/3}$. Here $v_{\rm sh,0}$ is the initial velocity of the shock front for the blast wave propagating into the external medium. The postshock magnetic field is $B = (8\pi\epsilon_B e_{\rm int})^{1/2}$, where $e_{\rm int} = 2\rho_{\rm ext}v_{\rm rel}^2$ and $\epsilon_B = 0.1\epsilon_{B,-1}$ is the fraction of the postshock internal energy in the magnetic field. The number of synchrotron-emitting electrons is $N_e = \xi_e M/m_p$, where $M = f_b(4\pi/3)\rho_{\rm ext}R^3$ and f_b is the beaming factor (i.e., the fraction of the total solid angle occupied by the outflow). Finally, $F_{\nu,\max} = N_e P_{\nu,\max}/4\pi d^2$, where $P_{\nu,\max} \approx P_{\rm syn}/\nu_{\rm syn}$, $P_{\rm syn}(\gamma_e) = (4/3)\sigma_{\rm T}c(B^2/8\pi)\gamma_e^2$, and $\nu_{\rm syn}(\gamma_e) = eB\gamma_e^2/2\pi m_e c$. The observed spectral slope in the radio suggests that we are in the spectral power-law segment $\nu_m < \nu < \nu_c$, where $\nu_m = \nu_{\rm syn}(\gamma_m)$ and ν_c is the cooling break frequency. Thus, we find

$$F_\nu = 4.2f_b g n_0^{3(p+1)/20}E_{46}^{(11+p)/10}\epsilon_{e,-1}\left(\frac{\epsilon_B}{0.002}\right)^{(p+1)/4}d_{15}^{-2} \times\left(\frac{\nu}{8.5\ {\rm GHz}}\right)^{(1-p)/2}\left(\frac{t}{33\ {\rm days}}\right)^{-3(p+1)/10}\ {\rm mJy} \quad (4)$$

at $t > t_{\rm dec}$, while $F_\nu(t < t_{\rm dec}) \approx (t/t_{\rm dec})^3 F_\nu(t_{\rm dec})$.

The parameter values in equation (4) were chosen to match the observed flux at the peak of the rebrightening, $t_{\rm dec} \approx t_p \approx$ 33 days. This demonstrates that an energy of $\sim f_b 10^{46}$ ergs, comparable to that in the GF (if it were emitted into a similar solid angle as the outflow), can be accommodated for reasonable values of the microphysical parameters and the external density. Taking into account the relation $n_0 \approx 0.26d_{15}^{-5}E_{46}$ derived

in § 2.2, we find that the requirement that the energy in relativistic electrons and in the magnetic field does not exceed equipartition, $\epsilon_e,\epsilon_B \lesssim 0.3$ (0.5), gives $E_{44} \gtrsim 7.5 d_{15}^{2.5}$ ($4.0 d_{15}^{2.5}$), where $E_{44} = E/(10^{44}$ ergs), consistent with the conclusions of Gelfand et al. (2005). For a wide one-sided jet of half-opening angle $\theta_0 \approx 0.5$ rad, $f_b = (1 - \cos\theta_0)/2 \approx 0.06$, while $E/n_{\rm ext}$ grows by a factor of $\sim 2^5$, where E is the isotropic equivalent energy. Altogether, we obtain for the true energy $E_{44} \gtrsim 5.7 d_{15}^{2.5}$ ($3.4 d_{15}^{2.5}$), as well as $n_0 \gtrsim 7.4\times10^{-3} d_{15}^{-2.5}$ ($4.4\times10^{-3} d_{15}^{-2.5}$) and $M_{\rm ej,24} \gtrsim 9.9 d_{15}^{0.5}$ ($5.9 d_{15}^{0.5}$), where $M_{\rm ej,24} = M_{\rm ej}/(10^{24}$ g).

Finally, we estimate the expected flux at the end of the collision between the ejecta and the external shell, at $\sim t_{\rm col}$. The external shell is accelerated to $\beta_f \approx \beta_{\rm ej}$ while the ejecta are only slightly decelerated, so that the shock going into the external shell is stronger and likely to dominate the emission. The volume of the shell, $4\pi\eta R_{\rm ext}^3$, where $\eta = \Delta R/R_{\rm ext} = 0.1\eta_{-1}$, is reduced by a factor of 4 due to shock compression, and its internal energy is a fraction $M_{\rm ext}/M_f \approx M_{\rm ext}/M_{\rm ej} \approx 0.007 t_{\rm col,5}^3$ of the total energy E. Under similar assumptions as above,

$$F_\nu(t_{\rm col}) \approx 80 f_b g^{p-1} \eta_{-1}^{-(p+1)/4} E_{46}^{(5+p)/4} \epsilon_{e,-1}^{p-1} \epsilon_{B,-1}^{(p+1)/4} d_{15}^{(5p-27)/4} \times \left(\frac{\nu}{8.5\ {\rm GHz}}\right)^{(1-p)/2} t_{\rm col,5}^3\ {\rm mJy}, \quad (5)$$

in rough agreement with the extrapolation to $t_{\rm col} \sim 5$ days of the observed flux, $F_{\nu=8.5\ {\rm GHz}} = 53$ mJy, at the first epoch, $t_{\rm I} = 6.9$ days (Cameron & Kulkarni 2005; Gaensler et al. 2005).

For the parameter values used in equation (5) we obtain $\nu_m \sim 1$ MHz, $\nu_{\rm sa} \sim 50$ MHz, and $\nu_c \sim 10^{17}$ Hz at $t_{\rm col} \sim 5$ days, where $\nu_{\rm sa}$ is the self-absorption frequency, so that the radio frequencies are well within the assumed power-law segment of the spectrum. The low value we obtain for $\nu_{\rm sa}$ is consistent with the lack of a change in the spectral slope down to 240 MHz (Cameron et al. 2005). Soon after the shock finishes crossing the shell, the electron power-law energy distribution extends up to $\gamma_{\rm max} \sim \gamma_c(t_{\rm col}) \sim 10^6$. Thereafter, adiabatic cooling takes over, and $\gamma_{\rm max} \propto t^{-2/3}$ while $B \propto t^{-1}$, so that $\nu_{\rm syn}(\gamma_{\rm max}) \sim \nu_c(t_{\rm col})(t/t_{\rm col})^{-7/3}$. The emission from the shocked external medium starts to dominate at $t \approx 25$ days, i.e., $t/t_{\rm col} \sim 5$, and hence at that time $\nu_{\rm syn}(\gamma_{\rm max}) \gtrsim 10^{15}$ Hz is well above the radio.

4. DISCUSSION

We have described a dynamical model for the interaction with the surrounding medium of the outflow during the 2004 December 27 giant flare (GF) from SGR 1806−20. This model nicely accounts for the observed radio light curves and spectrum as well as for the evolution of the source size with time. Using a simple analytic model, we have shown that the bulk of outflow from the GF could not have been highly relativistic and was instead only mildly relativistic, with an average velocity of $v/c \lesssim d_{15}(1 + d_{15}^2)^{-1/2} \sim 0.7$, similar to the observed roughly constant expansion velocity over the first month or so, taking into account the one-sided wide jet that is suggested by the radio data (Taylor et al. 2005).[12]

A major ingredient in our dynamical model is an external shell at a distance of $\sim 10^{16}$ cm from the SGR. Such an external shell might naturally be formed by the bow shock due to the SGR's quiescent wind and its supersonic motion relative to the external medium (Gaensler et al. 2005). A bow shock origin of the external shell has interesting implications. The bow shock stand-off radius is $R_{\rm bs} = 9.0\times10^{15} L_{34.5}^{1/2} n_0^{-1/2} v_{250}^{-1}$ cm, where $v_* = 250 v_{250}$ km s^{-1} is the velocity of SGR 1806−20 relative to the external medium and $L = 10^{34.5} L_{34.5}$ ergs s^{-1} is its spin-down luminosity.[13] In our scenario, $2R_{\rm ext}$ (the radius for a one-sided outflow) is $\sim(1-2)R_{\rm bs}$, i.e., $R_{\rm bs} \sim (1-2)R_{\rm ext}$ where $R_{\rm ext} \approx 6.4\times10^{15} t_{\rm col,5} d_{15}$ cm, which is the case for our fiducial parameters. Lower limits on the energy, $E \gtrsim 10^{44.5}$ ergs, and mass, $M_{\rm ej} \gtrsim 10^{24.5}$ g, of the outflow, and on the external density, $n_{\rm ext} \gtrsim 10^{-2}$ cm^{-3} have been derived in § 3 (see also Gelfand et al. 2005). The values of E, $M_{\rm ej}$, and $n_{\rm ext}$ scale linearly with each other; $E \sim 10^{46.5} n_0$ ergs and $M_{\rm ej} \sim 10^{26.5} n_0$ g. Note, however, that the minimal allowed density, $n_0 \sim 10^{-2}$, requires $v_* \sim 2500$ km s^{-1} and a similar kick velocity for SGR 1806−20 at its birth. While this is an extremely high kick velocity for typical radio pulsars, magnetars might have a significantly higher kick velocity than ordinary neutron stars, which might approach such high values (Duncan & Thompson 1992; Thompson & Duncan 1995). A lower kick velocity would suggest that the true values of E, $M_{\rm ej}$, and $n_{\rm ext}$ are larger than their lower limits by a factor of $\sim 100 n_0 \sim 100 v_{250}^{-2}$.

An alternative mechanism for producing the external shell is the ejection of a faster (and likely highly relativistic) component of the ejecta that carries a small fraction, f, of its total energy, just before (or in a slightly different direction relative to) the main part of the ejecta, which carries most of its energy and is only mildly relativistic. The first component may be naturally identified with the matter that is coupled to the radiation in the initial spike of the GF, which is expected to reach a highly relativistic Lorentz factor (Nakar et al. 2005). In order to obtain the ratio $R_{\rm dec}/R_{\rm ext} \sim 4-5$ that is inferred from observations, this would require $f \sim (R_{\rm dec}/R_{\rm ext})^{-3} \sim 10^{-2}$, i.e., that the ultrarelativistic component would carry $\sim$1% of the total energy in the outflow.

The fact that most of the energy in the outflow was in mildly relativistic ejecta implies that the bulk of the ejecta was not coupled to the radiation of the initial spike. This could occur if the bulk of the outflow and of the radiation came out in different directions (either in small local patches, or within some global, possibly concentric structure, as illustrated in Figs. 1*b* and 1*c*, respectively). Thus, it is not even obvious whether they occupied a comparable solid angle, which is important when trying to compare their true energies.

Our line of sight must have been in a relatively baryon-poor (and radiation-rich) region, not only in order to see a bright initial spike, but also since otherwise the high optical depth of the electrons associated with the baryons in the outflow would have obscured the first $\sim$30 s of the GF tail emission. This can be seen as follows. If a shell of mildly relativistic proton-electron plasma with velocity v_0 and isotropic equivalent mass $M_{\rm ej,iso}$ is ejected during the initial spike, at $t \approx 0$, then radiation emitted at time t after the initial spike would reach this shell at a radius $R(t) = v_0 t/(1 - v_0/c)$. The shell becomes optically thin to the radiation from the tail of the GF at time t_* when $\tau_T(t_*) = M_{\rm ej,iso}\sigma_{\rm T}/[m_p 4\pi R^2(t_*)] = 1$, i.e., at $t_* = (1 - v_0/c) v_0^{-1} (M_{\rm ej,iso}\sigma_{\rm T}/4\pi m_p)^{1/2}$. This gives $t_* \gtrsim 25$ s from the lower limits we obtain

[12] The local expansion velocity is highest along the jet axis. The observed axis ratio of $\sim 2:1$ for the radio image (Gaensler et al. 2005; Taylor et al. 2005) sets a lower limit on the true axis ratio of the emitting region.

[13] Before 1999 $L \approx 8\times10^{33}$ ergs s^{-1}, while by 2001 and until before the December 27th GF it leveled off at $L \approx 4.5\times10^{34}$ ergs s^{-1} (Woods et al. in preparation). The dynamical timescale for the bow shock is $t_{\rm bs} \sim R_{\rm bs}/v_* = 11.4 L_{34.5} n_0^{-1/2} v_{250}^{-2}$ yr. In our scenario, $R_{\rm bs} \sim (1-2)R_{\rm ext}$ so that $t_{\rm bs} \sim 12 t_{\rm col,5} d_{15} v_{250}^{-1}$ yr. Since the spin-down rate of SGR 1806−20 increased by a factor of $\sim$5 several years before the GF, the steady state assumption for the bow shock is not valid for $v_{250} \lesssim 2-3$. As a rough guide, one might still use the results for a steady wind (Wilkin 1996), with the average spin-down luminosity over a period $t_{\rm bs}$. The exact shape of the bow shock could, however, be somewhat different than that of a steady wind.

for $M_{\rm ej,iso}$ and for $\beta_{\rm min} \approx 0.7$ for a one-sided outflow (a similar result is obtained for the spherical case). The presence of $e^{\pm}$ pairs in the outflow or a large mass or velocity of the ejecta would only increase t_*.

In order for the highly relativistic ejecta to form the external shell into which the mildly relativistic ejecta collides, the two components must have a significant overlap in solid angle by the time of the collision, i.e., after the ultrarelativistic component decelerates to Newtonian velocities. This could occur if the two components form small patches, rather than a large-scale coherent structure (such as a baryon-rich core surrounded by a baryon-poor and radiation-rich outer region). Alternatively, if the external shell was created by the bow shock, then an energy ratio of $f \lesssim 10^{-2}$ is required in order for the highly relativistic component not to alter the radio emission considerably. This would be consistent with the very low energy in the ultrarelativistic component that is expected for a pure pair plasma (or for a very low baryon loading; Nakar et al. 2005).

For a wide one-sided jet we find that the lower limit on the isotropic equivalent kinetic energy in the outflow, $\gtrsim 5 \times 10^{45} d_{15}^{2.5}$ ergs, is only a factor of $\sim(3-4) d_{15}^{-0.5}$ smaller than the isotropic equivalent energy radiated in the GF itself. This suggests that the two isotropic equivalent energies are comparable. If the solid angles occupied by the baryon-rich (radiation-poor) and by the radiation-rich (baryon-poor) regions are comparable (which is not at all obvious), then this would suggest that the true energies in the GF itself and in the kinetic energy of the outflow are of the same order.

A much dimmer radio afterglow was detected following the 1998 August 27 GF from SGR 1900+14 (Frail et al. 1999), which, despite the much sparser data, shows similarities to the radio afterglow discussed here. This suggests that our model might be applicable more generally. The spin-down luminosity L of the two SGRs is comparable, and so is the time at which the light curve started to decay steeply ($\sim$9–10 days), suggesting that $R_{\rm bs}$ in each case is not very different. This would imply a similar $n_{\rm ext} v_*^2$. Under these assumptions, the large difference in the radio luminosity (by a factor of $\sim$500) would be mainly a result of the much larger energy content carried by the outflow of SGR 1806−20 immediately after the GF.

This research was supported by US Department of Energy under contract DE-AC03-76SF00515 (J. G.) and by NASA through a *Chandra* Postdoctoral Fellowship award PF3-40028 (E. R.-R.). The software used in this work was developed in part by the DOE-supported ASCI/Alliance Center for Astrophysical Thermonuclear Flashes at the University of Chicago. Computations were performed on the IAS Scheide computer cluster. B. M. G. and J. D. G. were supported by NASA through LTSA grant NAG5-13032. The National Radio Astronomy Observatory is a facility of the National Science Foundation operated under cooperative agreement by Associated Universities, Inc.

REFERENCES

Cameron, P. B., & Kulkarni, S. R. 2005, GCN Circ. 2928, http://gcn.gsfc.nasa.gov/gcn/gcn3/2928.gcn3
Cameron, P. B., et al. 2005, Nature, 434, 1112
Corbel, S., & Eikenberry, S. S. 2004, A&A, 419, 191
Duncan, R. C., & Thompson, C. 1992, ApJ, 392, L9
Frail, D. A., Kulkarni, S. R., & Bloom, J. S. 1999, Nature, 398, 127
Frail, D. A., Waxman, E., & Kulkarni, S. R. 2000, ApJ, 537, 191
Gaensler, B. M., et al. 2005, Nature, 434, 1104
Gelfand, J. D., et al. 2005, ApJ, 634, L89
Granot, J., Nakar, E., & Piran, T. 2003, Nature, 426, 138
Hurley, K., et al. 2005, Nature, 434, 1098
Kouveliotou, C., et al. 1998, Nature, 393, 235
McClure-Griffiths, N. M., & Gaensler, B. M. 2005, ApJ, 630, L161
Nakar, E., Piran, T., & Sari, R. 2005, preprint (astro-ph/0502052)
Palmer, D. A., et al. 2005, Nature, 434, 1107
Taylor, G. B., et al. 2005, ApJ, 634, L93
Thompson, C., & Duncan, R. C. 1995, MNRAS, 275, 255
Wilkin, F. P. 1996, ApJ, 459, L31